

05

## Spectral-generation properties and mechanism of formation of intercalated nanocomplexes dye–cyclodextrin

© S.S. Anufriick, S.N. Anuchin, V.V. Tarkovsky

Yanka Kupala State University of Grodno,  
230023 Grodno, Belarus

e-mail: anufriick@grsu.by

Received December 22, 2021

Revised March 17, 2022

Accepted March 17, 2022

Spectral-generation properties and the mechanism of formation of „dye-cyclodextrin“ inclusion complexes for dyes of different classes (rhodamine 6G, phenalemine 160, cresyl violet) with  $\beta$ -cyclodextrin were studied. The effect of functional groups in the structure of dye molecules on the spectral, generation, and photochemical properties of their inclusion complexes has been studied by electron and IR spectroscopy. It has been shown that the formation mechanism consists in the entry into the  $\beta$ -CD cavity of only individual functional groups and substituents of dye molecules. In this case, micellar complexes consisting of several cyclodextrin molecules and dye molecules and partially intercalated complexes can be formed. The AFM method showed that the characteristic sizes of the formed nanocomplexes are 100–600 nm.

**Keywords:** laser dyes,  $\beta$ -cyclodextrin, inclusion complexes, lasing spectral characteristics, FT-IR spectroscopy, photostability.

DOI: 10.21883/EOS.2022.08.54768.3065-21

### Introduction

One of the problems that limit the practical applications of dye lasers (DL) refers to photodecay of their molecules leading to insufficient useful life of active media of that class. It is especially relevant for lamp pumping dye lasers, with quite hard UV radiation in the pumping light. Under pumping light organic molecules are subjected to reversible or irreversible photodecay, whose products make considerable contributions into the losses in the active medium intensification.

Embodiment of opportunities of the dye laser practical applications relates to further improvement of their generation parameters, depending, first of all, on the dye solution specifications. Water is the most preferable as a solvent, because, when excited, it has the least thermal and optical distortions. However, dimerization and aggregation of dye molecules takes place in pure aqueous solutions, thus sharply decreasing the generation efficiency and the useful life [1].

In order to eliminate the aggregation and dimerization effect, it is necessary to protect the dye molecules against aqueous solvate shell, thus decreasing the losses caused by photodecay and the pumping-induced absorption.

Earlier, the authors of papers [2–7] demonstrated that in aqueous medium cyclodextrins (CD) are promising additives, whose molecules have toroidal shape and cavity, where dye molecules could enter into.

Provided that geometrical sizes of dye molecules and cyclodextrin cavity are taken correctly, one may form „guest–host“ inclusion complexes in the solution, enabling

total protection of the dye against unfavorable effects from solvent and UV pumping radiation.

The dye molecules could form inclusion complexes with cyclodextrin molecules while staying on the internal hydrophobic cavity of CD, as well as forming associative complexes with external hydrophilic enclosure of cyclodextrin via intermolecular hydrogen bonds.

Cyclodextrins forming the inclusion complexes with organic molecules can modify their fundamental optical properties. The inclusion complex nanostructures (cavities) can be formed by mixing substances either in dry crystalline state, or as suspensions, or as solutions. Production of inclusion complexes was performed by thermal activation [5].

In cited papers, as well as in other publications, the authors studied the dye inclusion complexes with cyclodextrins in water, wherein the cyclodextrin concentration ( $\sim 10^2$ ) exceeded heavily the dye content. In such conditions the dye molecules are fully surrounded by CD molecules and their aggregation is possible. In addition, high concentration of CDs ( $\sim 10^{-2}$  M) significantly modifies physical and chemical properties of water and its positive properties as a solvent of laser media; it is what affected comparatively low generation efficiency [4].

Therefore, creation of new laser media based on intercalated complexes of dyes with cyclodextrins is of a high scientific and practical interest.

The objective of this paper is the study of spectral and generation properties of the molecule inclusion complexes of various classes of dyes: rhodamine 6G (R6G), phenalemine 160, and cresyl violet with  $\beta$ -cyclodextrin in water-ethanol solutions and determination of the formation mechanisms of such complexes.

Water-ethanol solutions were used for the following reasons. In ethanol solutions, as known, the generation efficiency of the majority of dyes is the maximum, however, thermal and optical distortions are high. Aqueous media are preferred in terms of spatial-angular and thermal optical characteristics, however, the most of laser dyes are insoluble in water and do not generate. To the contrary, cyclodextrins are soluble in water and virtually do not modify optical properties of water-ethanol solutions of dyes.

## Objects, conditions and experimental procedure

The studies used dyes and reagents of the following brands: rhodamine 6G (LC 5900) (manufacturer: Lambda Physik AG), phenalemine 160 (PN-70) (manufacturer: FSUE GNTs NIOPIK), cresyl violet (LC 6700) (manufacturer: Lambda Physik AG),  $\beta$ -cyclodextrin (C 4767) (manufacturer: Sigma-Aldrich Chemie GmbH).

First, the powder of  $\beta$ -CD was solved in distilled water to the required concentration, next, while mixed, ethanol solution of dye at specific concentration was added to make the required ratio of „water-ethanol“. The inclusion complexes formation was performed by heating the produced solution up to 60°C and with further slow cooldown to the indoor ambient temperature [5].

Molar ratio of dye and  $\beta$ -CD in the solution changed from 1 : 1 to 1 : 5, which corresponded to the concentration of  $10^{-4}$ – $5 \cdot 10^{-4}$  M. The ratio of water and ethanol components of the solution was 1 : 1.

The dyes for the experiment were selected in terms of a high generation efficiency and different sizes (types) of molecules. Since efficient inclusion could occur in case of correspondence of the linear size of dye molecule and the cyclodextrin cavity volume, the paper performed calculation of the volume of molecules of the used dyes and of the linear size of their functional (auxochromic) groups. The internal cavity volume of  $\beta$ -CD is  $262 \text{ \AA}^3$ , diameter —  $6.6 \text{ \AA}$ , and torus height —  $8 \text{ \AA}$  [5].

Efficiency of formation of the dye inclusion complexes with  $\beta$ -CD was determined by changes of their electronic absorption and fluorescence spectra, by IR absorption spectra and generation properties versus water-ethanol solutions of raw dyes. Absorption spectra were measured by means of the Specord 200 spectrophotometer (Analytik Jena, Germany). The fluorescence spectra were registered by means of the SOLAR CM2203 spectrophotometer (CJSC Solar, Belarus) when excited at the wavelength of the maximum of main absorption band of the compounds under study. The IR spectra were registered by using the Nicolet iS10 IR Fourier-spectrometer (ThermoFisher Scientific, USA).

Dimension parameters of intercalated dye nanocomplexes were studied by means of the NT-206 scanning probe microscope (ALC Microtestmachines, Belarus). The studied solutions of dye complexes with  $\beta$ -CD drops were applied

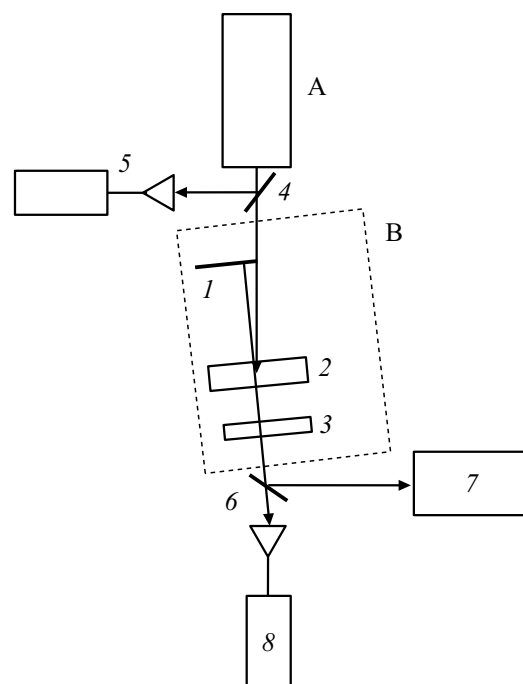


**Figure 1.** Experimental unit scheme: A —  $\text{Nd}^{3+}$ : YAG-laser; B — dye laser: 1, 3 — resonator mirrors, 2 — cell with the dye under study, 4, 6 — rotary glass plates, 5, 8 — energy meters IMO-2N, 7 — diffraction spectrograph DFS-13.

onto glass substrates and dried out at the indoor ambient temperature until evaporation is complete.

The generation characteristics of the water-ethanol solutions of dyes and their inclusion complexes were studied at quasilongitudinal coherent excitation by the 2nd harmonics of the LS-2147/3 Lotis Tii  $\text{Nd}^{3+}$ : YAG-laser (SP LOTIS TII, Belarus) at the unit [7], shown in Fig. 1.

## Results of experimental studies

First, the effect of cyclodextrin for the absorption spectra of water and water-ethanol solutions of rhodamine 6G was studied.

As we can see in Fig. 2, the rhodamine 6G water solution absorption spectrum (curve 1) contains two maxima: the short wavelength ( $\lambda = 500 \text{ nm}$ ) — dimeric one, and the longer wavelength ( $\lambda = 526 \text{ nm}$ ) — monomeric one — corresponding to various states of the dye molecule. With addition and increase of concentration in the  $\beta$ -CD solution in water medium, the dimeric maximum is gradually disappearing (curve 2). Subject to the fact that the R6G dimerization occurs due to interaction of carboethoxyphenyl group of benzene ring and xanthene nucleus oxygen atom [8], one may assume that the dimer dissociation process is related with the formation of the inclusion complex for carboethoxyphenyl group.

Similar effect is caused by ethanol addition into the R6G aqueous solution. Increase of the ethanol content

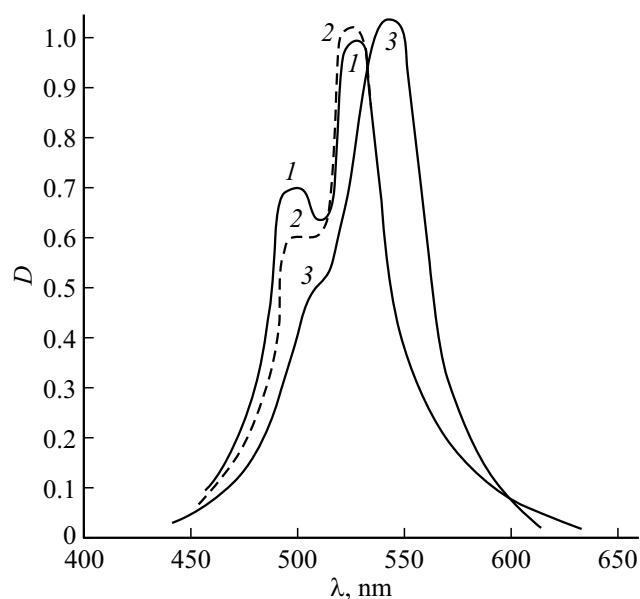


**Figure 2.** Absorption spectra of the R6G ( $10^{-4}$  M) (1) solutions and R6G complex with  $\beta$ -CD ( $2 \cdot 10^{-3}$  M) (2) in water, (1 : 1) R6G complex with  $\beta$ -CD ( $5 \cdot 10^{-4}$  M) in water-ethanol solution (3).

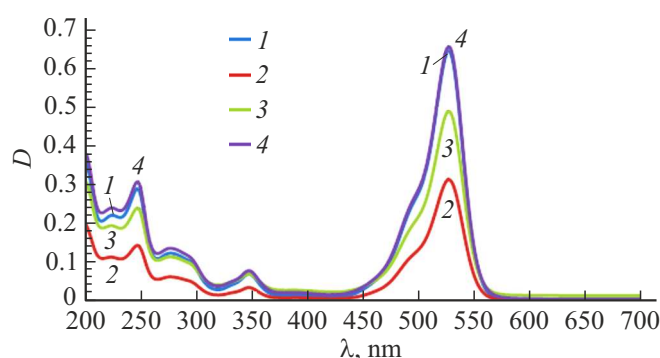


**Figure 3.** Absorption spectra of R6G water-ethanol solutions at the concentration ratio of  $\beta$ -CD and R6G 1 : 1 (1), 1 : 2 (2), 1 : 4 (3), 1 : 5 (4).

percentage (up to 50%) results in the decrease of the dimeric form intensity and monotonous long wavelength shift (by 15 nm) of the monomeric maximum, up to  $\lambda = 530$  nm, corresponding to the purely ethanol solution (Fig. 2, curve 3). The R6G fluorescence spectrum also undergoes long wavelength shift by 15 nm, and its quantum output rises from 10 to 95%.

Then, the effect of cyclodextrin concentration for the spectral properties of the R6G inclusion complex was studied. Fig. 3 shows R6G absorption spectra at different cyclodextrin content in the water-ethanol solution. As we can see in the figure, the increase of the cyclodextrin concentration from  $10^{-4}$  to  $5 \cdot 10^{-4}$  M virtually does not affect the position of the spectral bands.

However, as far as the  $\beta$ -CD content is increased in the solution (from 1 : 1 to 1 : 5 relative to R6G) the

absorbance (intensity) of the absorption bands is rising in UV and visible spectrum ranges. At the same time, the maximum absorbance corresponds to the CD concentration of  $5 \cdot 10^{-4}$  M. Further increase of the CD concentration has not changed the absorption spectrum of the complex. It is specific that for this concentration of  $\beta$ -CD intensity of main absorption maximum of R6G is the maximum.

While in the dry crystalline state, cyclodextrins have no high hygroscopic properties [9]. However, in the process of cyclodextrins crystallization from water solutions, the molecules of water are actively included into the torus cavity, as well as present in the crystalline structure of the substance, bonding with the external surface of the molecules. Under normal conditions, the specific number of the water molecules associated with one cyclodextrin molecule is: for the  $\alpha$ -cyclodextrin — 6.2 molecules, for the  $\beta$ -cyclodextrin — 9.6 molecules, for the  $\gamma$ -cyclodextrin — 14.2 molecules of water [10].

The structure of cyclodextrin crystalline is stabilized by intermolecular hydrogen bonds. In crystalline hydrate state the cyclodextrin molecule aggregates have a tubular or mesh-like shape and, due to different orientations, form needle-like or prism-like agglomerate particles. The crystalline shape depends on the degree of hydration. In case of dehydration, crystals turn to amorphous state [10, 11]. During the inclusion complexes formation, water molecules are partially displaced from the cyclodextrin torus cavity as a result of intrusion of the corresponding molecule of the „guest“ substance [9].

As noted in the paper [9], a specific number of the water molecules associated with the cyclodextrin molecule in its cavity may reach 14. This is why in water-ethanol solution the ethanol solvate shell can be preserved for the R6G molecules by the displacement of water molecules from the  $\beta$ -CD cavity, which could also explain the absence of shift of the studied spectra in aqueous solution. Intrusion of the R6G molecule may occur partially only, due to big differences in size of the dye molecule ( $V_{R6G} = 2564 \text{ \AA}^3$ ) and the cavity  $\beta$ -CD ( $262 \text{ \AA}^3$ ) [12].

Fig. 4 shows spectra of absorption (A) and fluorescence (B) of phenalemine 160 (I) and cresyl violet (II) in case of variation of the  $\beta$ -CD content in water-ethanol solution.

Comparison of the spectra of absorption and fluorescence of phenalemine 160 and cresyl violet shows that when  $\beta$ -CD is added (within 1 : 1 to 1 : 5) a minor long wavelength shift only takes place (by 2–3 nm) of the phenalemine 160 absorption spectrum. The absorption and fluorescence spectra of their inclusion complexes with  $\beta$ -CD are quite identical in terms of the shape and position to water-ethanol solutions. Wherein, increase of concentration of  $\beta$ -CD results only a minor expansion thereof.

The absence of three-dimensional substitutes in the phenalemine?160 molecule structure (the same aminogroup) and a high localization of charge on the phenalemine nucleus (additional benzene cycle) cause its weak intramolecular interaction with the  $\beta$ -CD, which affects a weak absorption spectrum shift.

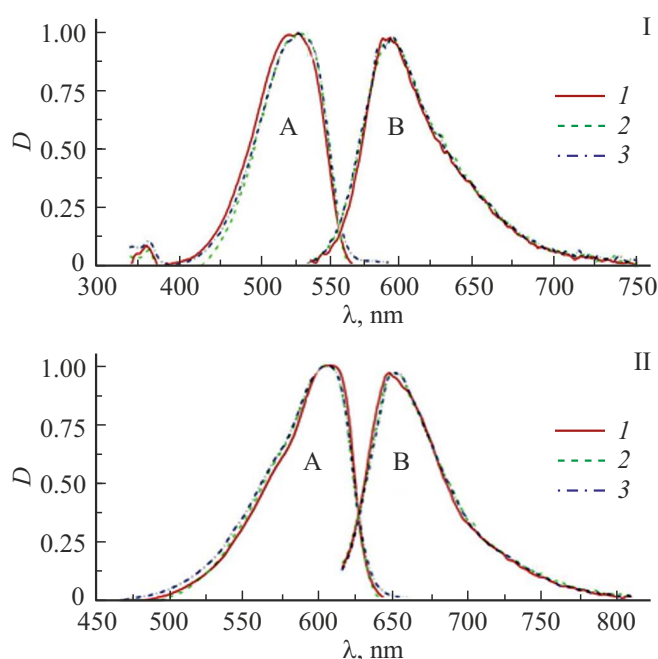


**Figure 4.** The spectra of absorption (A), and fluorescence (B) of phenalemine 160 (I) and cresyl violet (oxazine-9) (II) in water-ethanol solution (1);  $\beta$ -CD in the ratio of 1 : 1 (2);  $\beta$ -CD in the ratio of 1 : 5 (3).

In order to identify the mechanism of intercalated complexes formation of the dyes in question, their IR absorption spectra were studied. In order to calculate the molecular structure, the Becke–Lee–Yang–Parr hybrid functionality was applied (B3LYP) [13].

The DFT (Density Functional Theory) and the TDDFT (Time-Dependent Density-Functional Theory) were used as calculation methodologies. The Chemcraft 5.62 software tool, which allows visualization of three-dimensional structures of the studied molecules, was used for building structural formulas of the studied molecules and for the visualization of the outcome.

Fig. 5 shows IR spectra of the R6G absorption, its inclusion complex with  $\beta$ -CD and pure  $\beta$ -CD.

As we can see, several new bands appear in the IR spectrum of the R6G inclusion complex with  $\beta$ -CD: at 1030, 1150, and 2900  $\text{cm}^{-1}$ , typical for the  $\beta$ -CD. At that, a high decrease of intensity for all bands is observed. The frequencies corresponding to R6G, in the inclusion complex spectrum undergo bathochromic shift relative to its original position by 5–50  $\text{cm}^{-1}$ . At that, the most considerable shift is inherent to the band at 1078  $\text{cm}^{-1}$  (–48  $\text{cm}^{-1}$ ), corresponding to C–O–C symmetrical valent vibrations in aromatic ethers, to the band 1190  $\text{cm}^{-1}$  (–40  $\text{cm}^{-1}$ ), corresponding to various vibrations of aromatic rings, to the band 2942  $\text{cm}^{-1}$  (–42  $\text{cm}^{-1}$ ), corresponding to valent vibrations of C–H-groups, and to the band 3354  $\text{cm}^{-1}$  (–64  $\text{cm}^{-1}$ ), corresponding to valent vibrations of the groups –N–H.

The inclusion complex spectrum has virtually all smoothed bands, which are typical for the R6G IR spec-

trum, corresponding to various vibrations of the fluoronic nucleus. Vibrations of the ether group and ethylic, amino-, and imino- end groups of R6G (3354, 2985, 2942, 1272, 1078  $\text{cm}^{-1}$ ) attenuate, which might indicate their intrusion into the cavity of  $\beta$ -CD and shielding (Table 1).

As it was noted before, with the molecule volume  $\sim 2564 \text{ \AA}^3$  R6G can enter the cavity of  $\beta$ -CD either of one of the ethylamine groups –NH–C<sub>2</sub>H<sub>5</sub> (length 8.16 Å, the width of 3.96 Å) with phenyl part of rhodamine (fluorone) nucleus (the width of 5.84 Å), or carboethoxyphenyl group –C<sub>6</sub>H<sub>5</sub>–COOC<sub>2</sub>H<sub>5</sub> (the width of 6.39 Å). The [8] shows that the R6G molecule can contain two isomers differing by spatial orientation of ethylamine groups, wherein the plane structure of the rhodamine nucleus persists, and the carboethoxyphenyl group is oriented perpendicular to the plane of the molecule backbone. Due to that, a complete intrusion of the carboethoxyphenyl group of the R6G molecule is possible, because its linear dimensions (the width of  $\sim 6.39 \text{ \AA}$ ) is less than the  $\beta$ -CD torus cavity diameter (8.4 Å).

Therefore, the complex formation may occur due to intrusion of auxochromic groups from various sides of the rhodamine nucleus into two molecules of  $\beta$ -CD, and carboethoxyphenyl group — into the third molecule of  $\beta$ -CD, which results in a stable equilibrium state of the complex and is evidenced by the absence of shift of electronic spectra of absorption and fluorescence and higher (3–5 times) concentration of cyclodextrin.

Subject to the results of analysis of the electron and IR absorption spectra (shift of vibrating bands of relevant groups) and the data of calculations of the molecular structure, probable view of the intercalated R6G complex with  $\beta$ -CD can be represented by micelle, whose external shell is formed by the  $\beta$ -CD molecules in water, and the internal one contains the R6G molecule, solvated by ethanol and partially intruded into the cyclodextrin macrocycle (Fig. 6). Stability of the complex is ensured by hydrophobic and hydrophilic interactions, due to the formation of hydrogenic and van der Waals bonds. Joining of other cyclodextrin molecules by the hydrophilic shell to the inclusion complex (IC) is not excluded.

Fig. 7 shows IR absorption spectrum of phenalemine 160, its inclusion complex and  $\beta$ -CD. As we can see, new bands appear in the phenalemine 160 inclusion complex spectrum at the frequencies of 1020 and 2906  $\text{cm}^{-1}$ , which are typical for  $\beta$ -CD. At that, a decrease of intensity in the IC spectrum for all bands is observed. The bands corresponding to phenalemine 160, in the inclusion complex spectrum undergo both hypsochromic and bathochromic shift relative to its original position. The most significant high-frequency shift is inherent to the band at 3165  $\text{cm}^{-1}$  (+23  $\text{cm}^{-1}$ ), corresponding to the aminogroup vibrations. For the band of 2994  $\text{cm}^{-1}$ , bathochromic shift by –88  $\text{cm}^{-1}$ , related with valent vibrations of phenalemine nucleus, is observed. The observed high-frequency shift of these valent vibration bands could be caused by intermolecular interaction with  $\beta$ -CD as a result of formation of hydrogen bonds with the

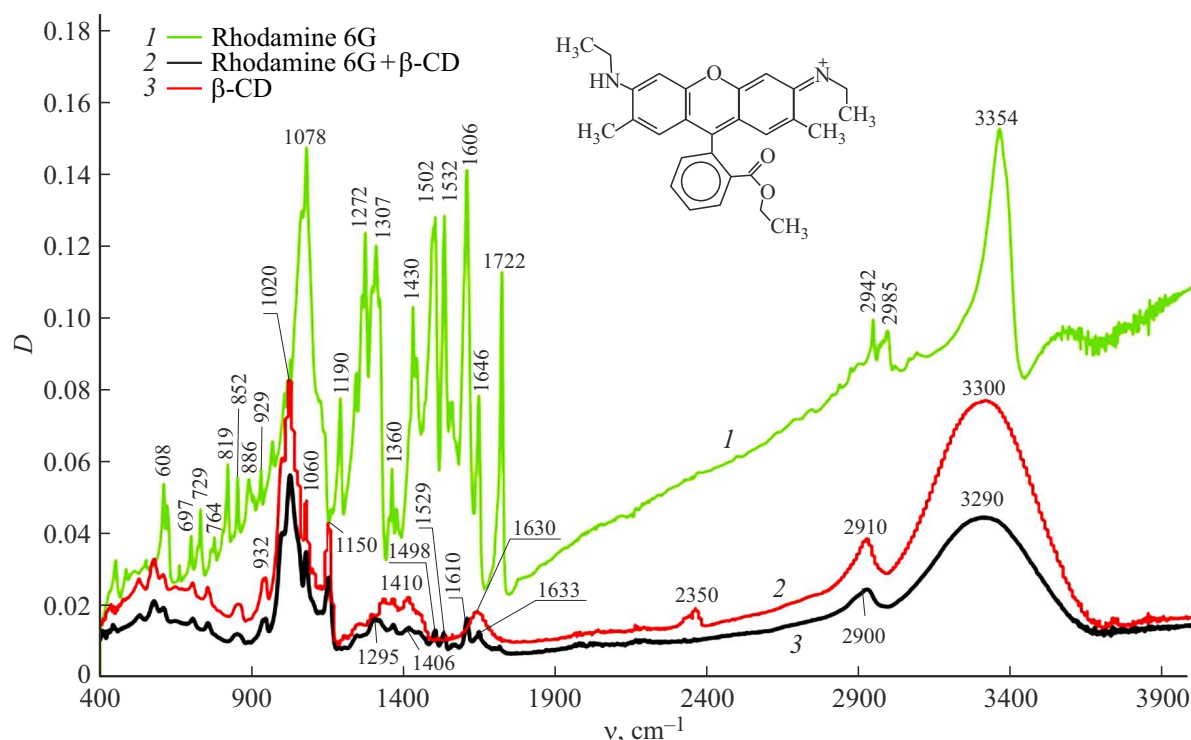


**Figure 5.** IR absorption spectra of R6G (1), of the R6G inclusion complex with  $\beta$ -CD (2),  $\beta$ -CD (3).

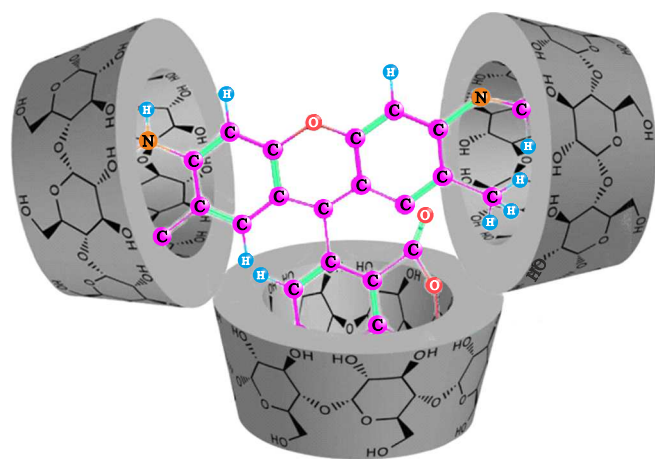


**Figure 6.** Probable 3D-model of the micellar complex of R6G with  $\beta$ -CD.

external shell of CD. A significant decrease of frequencies of valent vibrations of the phenalemine nucleus may indicate intrusion of its part into the cyclodextrin molecule cavity.

Vibrations of the carbonyl group of phenalemine?160 ( $1861\text{ cm}^{-1}$ ) attenuate, which can be related with intrusion thereof into the cavity of  $\beta$ -CD and shielding (Table 2).

Complete intrusion of the phenalemine 160 molecule into the cavity of  $\beta$ -CD is limited to steric factors due to high dimensions of the phenalemine nucleus. This is why complex formation may occur due to partial intrusion of

carbonyl group with a part of the dye molecule nucleus into the cyclodextrin cavity and formation of hydrogen bonds between the aminogroup with external hydrophilic sphere  $\beta$ -CD. It is also confirmed by a small shift of the absorption spectrum (Fig. 4, 1A). This is why the most probable model of the IC of the phenalemine 160 with  $\beta$ -CD can be the one shown in Fig. 8.

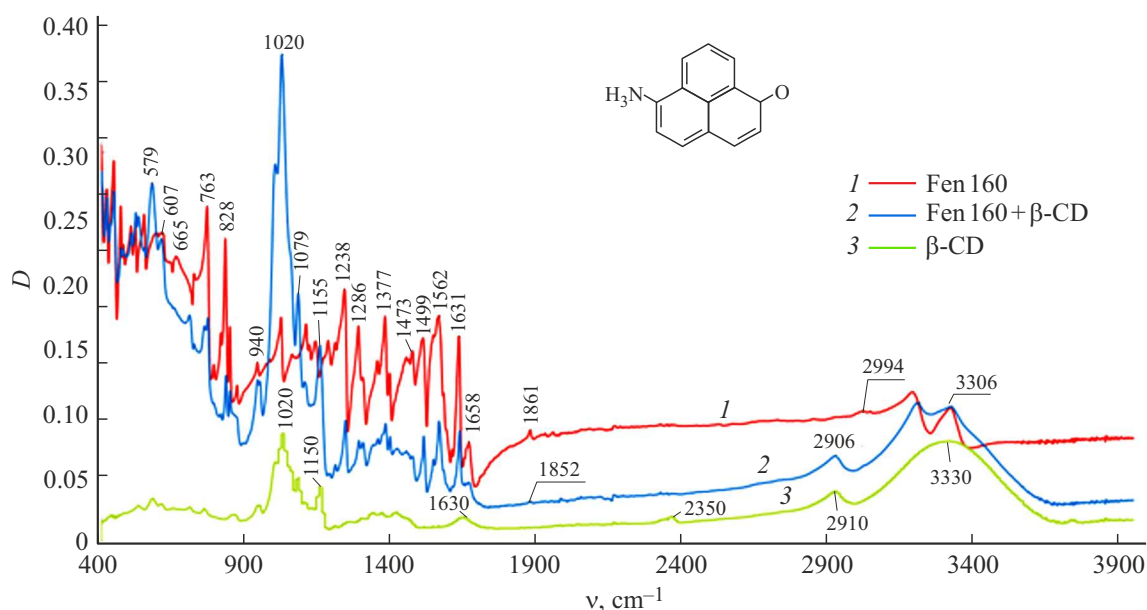
Fig. 9 shows IR absorption spectra of cresyl violet,  $\beta$ -CD and inclusion complex.

The bands corresponding to cresyl violet, in the inclusion complex spectrum undergo a weak (up to  $5\text{ cm}^{-1}$ ) bathochromic shift relative to its original position. The same as for phenalemine 160, several new bands typical for  $\beta$ -CD appear in the IR spectrum of the cresyl violet — at  $1000$  and  $2900\text{ cm}^{-1}$ . At that, minor drop of the bands intensity is observed within the range  $800\text{--}1600\text{ cm}^{-1}$ , corresponding to various oscillations of the cresyl violet molecule. A broad structured band in the low-frequency region of the spectrum  $400\text{--}600\text{ cm}^{-1}$  is caused by vibrations of perchlorate-ion and a part of the dye molecule corresponding to  $\beta$ -naphthalene. Formation of the inclusion complex results in an increase of intensity of that band and its structuring (as for  $\beta$ -CD), which can be related with vibrations of external shell of cyclodextrin. The cyclodextrin-specific vibration band in the region of  $3000\text{--}3500\text{ cm}^{-1}$  when the inclusion complex is formed is amplified by two maxima, which correspond to valent oscillations of auxochromic groups of cresyl violet ( $-\text{NH}_2$ ,  $=\text{NH}$ ). Rise of their intensity and preservation of the shape of bands similar to the spectrum of cresyl violet indicates that these data of functional group



**Table 1.** Assignment of the R6G IR spectrum vibration bands and its inclusion complex with the  $\beta$ -CD

| Frequency $\nu$ , $\text{cm}^{-1}$ |                 |                  | Assignment of vibrations  |
|------------------------------------|-----------------|------------------|---|
| R6G experiment                     | R6G theory [14] | R6G+ $\beta$ -CD |   |
| 3354                               | 3450–3300       | 3290             | Valent vibrations N–H   |
| 2985, 2942                         | 3000–2840       | 2900             | Valent vibrations C–H   |
| 1722                               | 1718            | 1740             | Vibrations of RCOH  |
| 1646                               | 1649            | 1633             | Vibrations of $\text{RCH}=\text{CH}_2$  |
| 1606                               | 1606            | 1610             | Vibrations of aromatic rings  |
| 1532                               | 1528            | 1529             | Vibrations of aromatic rings  |
| 1502                               | 1500            | 1498             | Vibrations of pyrylium derivatives  |
| 1430                               | 1433            | 1406             | Flat deformational vibrations C–H   |
| 1360                               | 1366            | 1359             | Deformational vibrations $\text{C}_2\text{H}_5$   |
| 1307                               | 1305            | 1295             | Wagging and torsional vibrations $\text{CH}_3$  |
| 1272                               | 1269            | 1270             | Asymmetrical valent vibrations of C–O–C in ethers   |
| 1190                               | 1187            | 1150             | Vibrations of aromatic rings  |
| 1078                               | 1090            | 1030             | Symmetrical valent vibrations of C–O–C in ethers  |
| 929                                | 930             | 932              | Vibrations of $\text{ClO}_3^-$  |
| 886                                | 886             | 886              | Vibrations of aromatic rings  |
| 852                                | 851             | 850              | Vibrations of monosubstituted aromatic rings with simple substitutes ( $\text{CH}_3$ , $\text{NH}_2$ , Cl etc.) |
| 819                                | 816             | —                | Vibrations of monosubstituted aromatic rings with simple substitutes ( $\text{CH}_3$ , $\text{NH}_2$ , Cl etc.) |
| 764                                | 768             | 770              | Vibrations of aromatic rings  |
| 729, 697                           | 1100–600        | 730              | $=\text{C-H}$ deformational out-of-plane vibrations   |

**Figure 7.** IR absorption spectra of phenalemine 160 (1), inclusion complex (2),  $\beta$ -CD (3).

are beyond the inclusion complex and excited by the molecule conjugation chain. It is also indicated by rise and bathochromic shift by  $20\text{ cm}^{-1}$  of the band maximum in the region of  $1580\text{ cm}^{-1}$ , corresponding to vibrations of aromatic rings of the cresyl violet nucleus (Table 3).

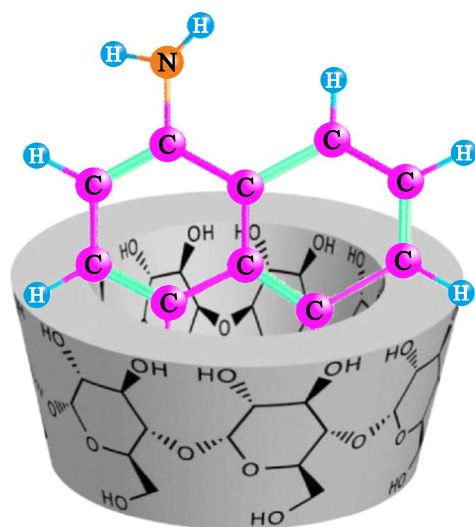
The IR spectrum of the inclusion complex of cresyl violet  $\beta$ -CD has also the bands (Table 3), which are typical for the IR spectrum of dye corresponding to vibrations of amino

end-groups and various types of vibrations of the molecule nucleus.

Since no attenuating vibrations of any parts of molecules of cresyl violet are observed, but a series of vibrating bands corresponding to the conjugation chain ( $\sim 700\text{--}1000\text{ cm}^{-1}$ ) is intensified, then one may assume that intermolecular interaction is performed due to intrusion only of the dye phenyl group into the cyclodextrin cavity.

**Table 2.** Assignment of the phenalemine 160 IR spectrum vibration bands and its inclusion complex with the  $\beta$ -CD [15]

| Fen 160<br>experiment | Frequency $\nu$ , $\text{cm}^{-1}$ |                      | Assignment of vibrations  |
|-----------------------|------------------------------------|----------------------|---|
|                       | Fen 160<br>theory                  | Fen 160+ $\beta$ -CD |   |
| 3306                  | 3500–3300                          | 3306                 | Valent vibrations of O–H<br>(hydrated salts)                      |
| 3165                  | 3500–3000                          | 3188                 | Valent vibrations N–H   |
| 2994                  | 3000                               | 2906                 | Valent vibrations C–H   |
| 1861                  | 1800                               | 1852                 | Valent vibrations C=O   |
| 1658                  | 1650                               | 1665                 | Valent vibrations C=O   |
| 1631                  | 1650                               | 1640                 | Valent vibrations C=C   |
| 1562                  | 1560                               | 1569                 | Deformational out-of-plane vibrations<br>aromatic ring vibrations |
| 1499                  | 1500                               | 1509                 | Symmetrical valent<br>vibrations =C–H                             |
| 1473                  | 1450                               | 1466                 | Scissoring vibrations of =C–H                                     |
| 1452                  | 1450                               | 1455                 | Scissoring vibrations of =C–H                                     |
| 1371                  | 1300                               | 1377                 | Vibrations of rings (nucleus)                                     |
| 1286                  | 1250–800                           | 1281, 1289           | Vibrations of rings (nucleus)                                     |
| 1238                  | 1250–800                           | 1244                 | Vibrations of rings (nucleus)                                     |
| 1170                  | 1250–800                           | 1150                 | Asymmetric vibrations<br>rings (nucleus)                          |
| 1165                  | 1250–800                           | 1155                 | Asymmetric vibrations<br>rings (nucleus)                          |
| 1016                  | 1100–600                           | 1020                 | deformational out-of-plane vibrations<br>vibrations =C–H          |
| 940                   | 940                                | 934                  | Vibrations of rings of derivatives of<br>benzene (C=C–C=O)        |
| 828                   | 820                                | 831                  | Valent out-of-plane vibrations<br>–C–N–                           |
| 763                   | 1100–600                           | 764                  | Deformational out-of-plane<br>vibrations =C–H                     |
| 607                   | 700–600                            | 609                  | Deformational weak vibrations<br>$\equiv$ C–H                     |
|                       | 700–600                            | 579                  | Deformational weak vibrations $\equiv$ C–H                        |

**Figure 8.** Probable 3D-model of the phenalemine 160 inclusion complex with  $\beta$ -CD.

Wherein the main conjugation chain — fluoronic nucleus of the molecule — is located beyond and the effect of cyclodextrin for such an inclusion complex is minimum, and it is instable himself.

The model of cresyl violet IC with  $\beta$ -cyclodextrin based on the above is shown in Fig. 10.

In order to identify specific dimensions of the formed nanocomplexes of dyes with  $\beta$ -CD their AFM images were studied. Fig. 11 shows AFM images of the studied inclusion nanocomplexes of dyes with  $\beta$ -CD.

As we can see, for R6G (Fig. 11,a) a cellular nanostructure is observed, which is formed by multiple oval particles with dimensions of  $\sim 500$ – $600$  nm and height up to  $600$  nm. These typical sizes could correspond to the earlier mentioned micelles of IC of R6G with  $\beta$ -CD (Fig. 6). AFM image of phenalemine 160 with  $\beta$ -CD (Fig. 11,b) contains coarse elongated aggregated conglomerates of pyramidal shape of micrometer size. These nanostructures correspond by size to aggregated molecules of  $\beta$ -CD (Fig. 11,d). For the complex of cresyl violet on AFM image

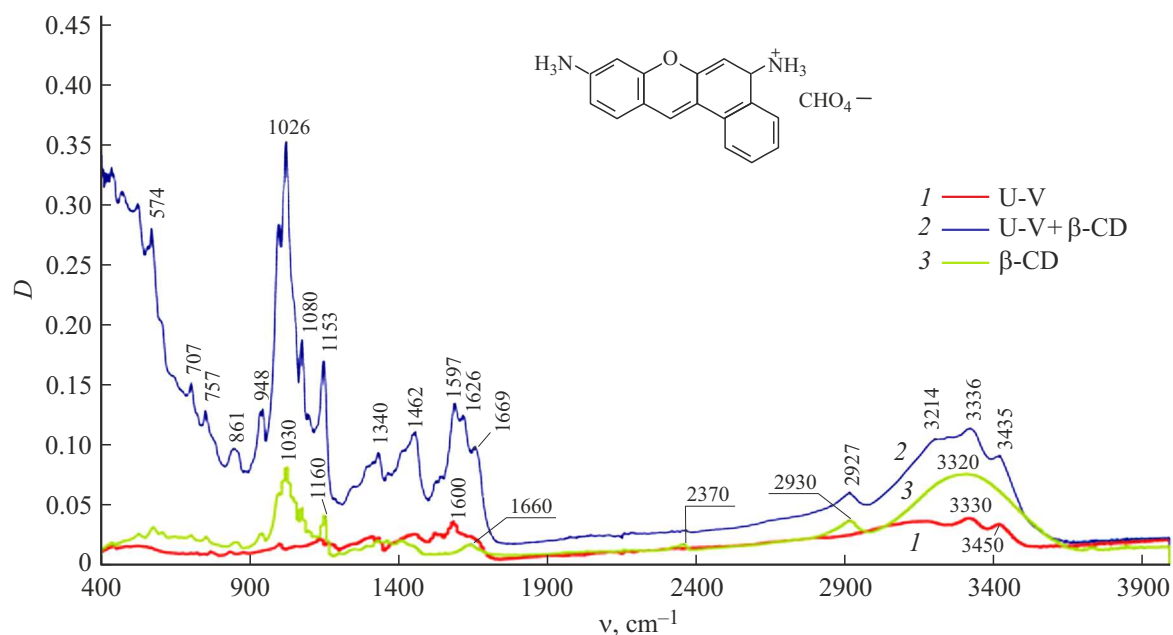


**Figure 9.** IR absorption spectra of cresyl violet (1), inclusion complex (2), and  $\beta$ -CD (3).

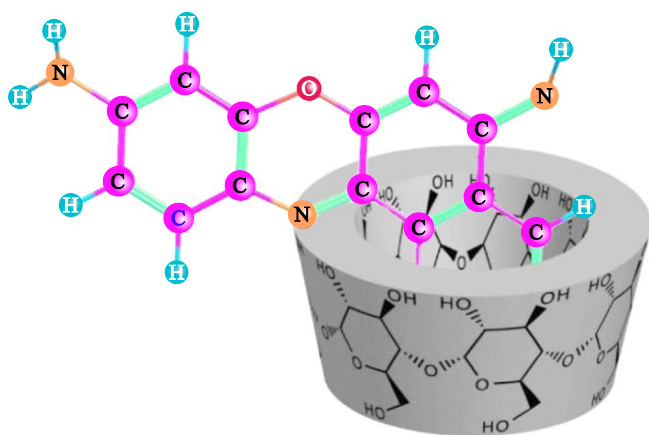


**Figure 10.** Probable 3D-model of the IC of cresyl violet with  $\beta$ -CD.

(Fig. 11, *c*) we can see individual spherical nanostructures with the dimensions  $\sim 400$  nm and elongated, consisting of chains ( $-1 - 1.5 \times 0.5 \mu\text{m}$ ), conglomerated nanoparticles (probably, inclusion complexes). For comparison, the image 11, *d* refers to the AFM image of pure  $\beta$ -CD. As we can see, the coating is quite homogeneous, but contains individual coarse annular ( $d \sim 4 \mu\text{m}$ ) and elongated ( $\sim 8 \times 2 \mu\text{m}$ ) formations with the height of  $\sim 300 - 400$  nm, probably corresponding to associated conglomerates of cyclodextrin molecules.

Next, we studied generation characteristics of the inclusion complexes of mentioned dyes depending on the water percentage and concentration of  $\beta$ -CD in solution (Fig. 12).

As we can see in the figure, the trend of dependence of the IC generation energy of R6G and phenalemine 160 on

the cyclodextrin concentration has the optimum at the 50% solution and cyclodextrin content of  $5 \cdot 10^{-4}$  M (curve 3). Dilution of ethanol with water up to the 50% solution has a minor effect for the generation efficiency of R6G and phenalemine 160, however, further decrease of the ethanol content results in a sharp decrease of the generation energy (Fig. 12, curve 4). The presence of optimum concentration of  $\beta$ -CD in the inclusion complex indicates participation of several cyclodextrin molecules in formation of micellar complex with the dye. However, further increase of concentration (over  $10^{-3}$  M)  $\beta$ -CD results in the fall of the generation energy. Possible cause could be the change of physical and chemical properties of the solution and the nature of complex formation (at high concentrations of CD) due to the formation of dimers, scattering and suppression of fluorescence [16].

The generation parameters of R6G, phenalemine 160, cresyl violet and their complexes with  $\beta$ -CD in water ethanol solutions are given in Table 4.

According to Table 4, the highest efficiency (71.4%) in pure ethanol solution corresponds to R6G, for phenalemine 160 it is 50%, and for cresyl violet — 25%.

In water-ethanol solution the maximum efficiency of generation — 71.4% was obtained for phenalemine 160, which, compared to the ethanol solution, has increased by 21.4%. For R6G and cresyl violet the generation efficiency has fallen by  $\sim 20$  and 50%, accordingly.

The increase of the phenalemine 160 generation efficiency in water-ethanol solution can be associated with the availability of carbonyl group molecule in the structure. Because of the water content in ethanol solution, hydrogen bonds generation and hydroxyl group formation in the molecule structure is possible due to intermolecular interactions, which ensures its better solubility. The generation



**Table 3.** Assignment of the cresyl violet IR spectrum vibration bands and its inclusion complex with the  $\beta$ -CD [15]

| Frequency $\nu$ , $\text{cm}^{-1}$ |             |                   | Assignment of vibrations                                  |
|------------------------------------|-------------|-------------------|---|
| Kr-V experiment                    | Kr-V theory | Kr-V+ $\beta$ -CD |   |
| 3450                               | 3500        | 3435              | Valent vibrations N–H                                     |
| 3330                               | 3000        | 3336              | Valent vibrations C–H                                     |
| 3000                               | 3000        | 321               | Valent vibrations C–H                                     |
| 2800                               | 3000–2840   | 2927              | Valent vibrations C=H                                     |
| 1655                               | 1600        | 1669              | Valent vibrations –C=C–                                   |
| 1630                               | 1630–1510   | 1626              | Vibrations of C=T<br>out-of-plane                         |
| 1600                               | 1630–1510   | 1597              | Out-of-plane<br>vibrations of C=N                         |
| 1520                               | 1630–1510   | 1521,1526         | Out-of-plane<br>vibrations of C=N                         |
| 1466                               | 1465        | 1462              | Plane vibrations of =C–H                                  |
| 1440                               | 1475–       | 1450              | Flat deformational<br>vibrations –C=C–H                   |
| 1346                               | 1390–1260   | 1340              | NO <sub>2</sub> Symmetrical<br>valent vibrations          |
| 1282                               | 1395–1265   | 1287              | Symmetrical deformational<br>vibrations of ring           |
| 1233                               | 1395–1265   | 1239              | Symmetrical deformational<br>vibrations of ring (nucleus) |
| 1151                               | 1300–1000   | 1147              | Valent asymmetrical<br>vibrations of ring (nucleus) C–O–C |
| 1101                               | 1170–1115   | 1088              | Valent vibrations<br>asymmetrical C–C                     |
| 1050                               | 1100–600    | 1022              | Deformational out-of-plane<br>vibrations =C–H             |
| 1016                               | 1100–600    | 1026              | Deformational out-of-plane<br>vibrations =C–H             |
| 940                                | 1100–600    | 948               | Deformational out-of-plane<br>vibrations =C–H             |
| 837                                | 1100–600    | 861               | Deformational out-of-plane<br>vibrations =C–H             |

**Table 4.** The generation parameters of R6G, phenalemine 160, cresyl violet and their complexes with  $\beta$ -CD in water ethanol solutions

| Name compounds  | Ethanol solution |              | Water-ethanol solution (1 : 1) |              |                      | Water-ethanol solution (1:1) with $\beta$ -cyclodextrin |              |                      |
|-----------------|------------------|--------------|--------------------------------|--------------|----------------------|---|--------------|----------------------|
|                 | $E_g$ , mJ       | $\eta_g$ , % | $E_g$ , mJ                     | $\eta_g$ , % | $\Delta\lambda$ , nm | $E_g$ , mJ  | $\eta_g$ , % | $\Delta\lambda$ , nm |
| Rhodamine 6G    | 100              | 71.4         | 83                             | 59.3         | 562–572              | 104   | 75.3         | 561–575              |
| Phenalemine 160 | 70               | 50           | 100                            | 71.4         | 603–630              | 85  | 60.7         | 598–614              |
| Cresyl violet   | 35               | 25           | 17                             | 12.1         | 636–648              | 24  | 17.1         | 631–641              |

efficiency decrease of R6G and cresyl violet is caused by specifics of their molecular structure and partial aggregation in water medium, which is also confirmed by less quantum outcome of fluorescence.

For the inclusion complex R6G with  $\beta$ -cyclodextrin in water-ethanol solution, the generation efficiency has risen up to 75%, exceeding the generation efficiency in pure ethanol solution (71.4%). Versus water-ethanol solution, the generation efficiency of the inclusion complex of R6G

with  $\beta$ -CD has also increased (by 16%). Increase of the energy generation of the IC R6G, as it was noted before, is associated with intrusion of its auxochromic substitutes into hydrophobic cavity  $\beta$ -CD and shielding of external hydrophilic shell of cyclodextrin. For the IC with phenylamine 160 and cresyl violet, minor change of the generation efficiency is observed (by 5–10%), which can be associated with the partial intrusion of their functional groups into the cavity of  $\beta$ -CD.

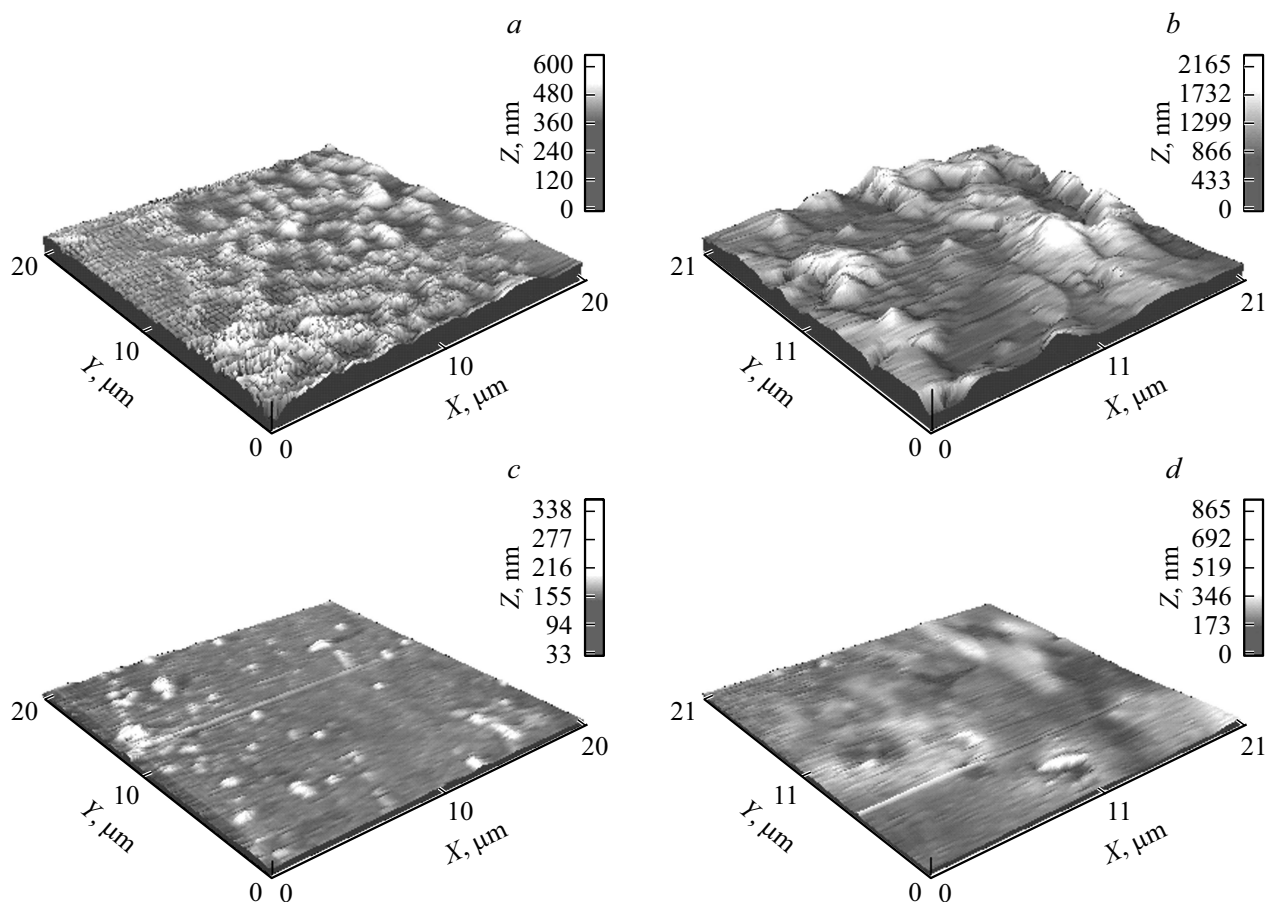


**Figure 11.** The AFM images of the inclusion complexes of R6G (a), phenalemine 160 (b), cresyl violet (c) with the ratio „dye–cyclodextrin“ — 1 : 3 and pure  $\beta$ -CD (d).

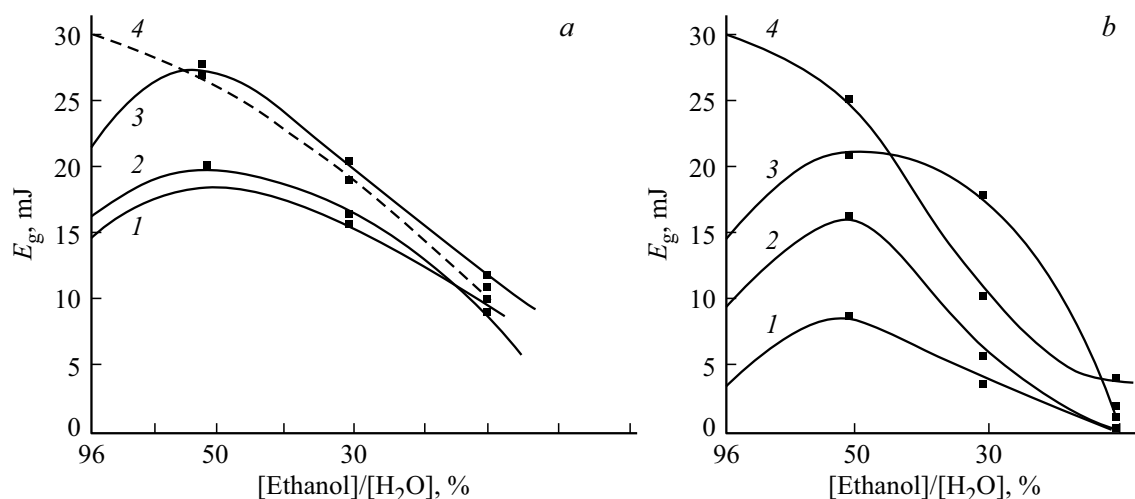


**Figure 12.** Dependence of the energy of inclusion complexes generation R6G (a) and phenalemine 160 (b) on the water percentage and concentration  $\beta$ -CD: 1 —  $10^{-4}$  M; 2 —  $3 \cdot 10^{-4}$  M; 3 —  $5 \cdot 10^{-4}$  M; 4 — without  $\beta$ -CD.

The generation spectrum of IC R6G with  $\beta$ -CD has virtually not changed, and for the IC of phenalemine 160 and cresyl violet, a minor narrowing and shift towards short wavelength region (by 16 and 7 nm accordingly) are observed.

An important problem of dye lasers is also photodecay of the active medium molecules when excited by a powerful pumping radiation. As it was shown earlier [17,18], during the inclusion complex formation with a dye, the dye molecules shielding is possible by an external shell of

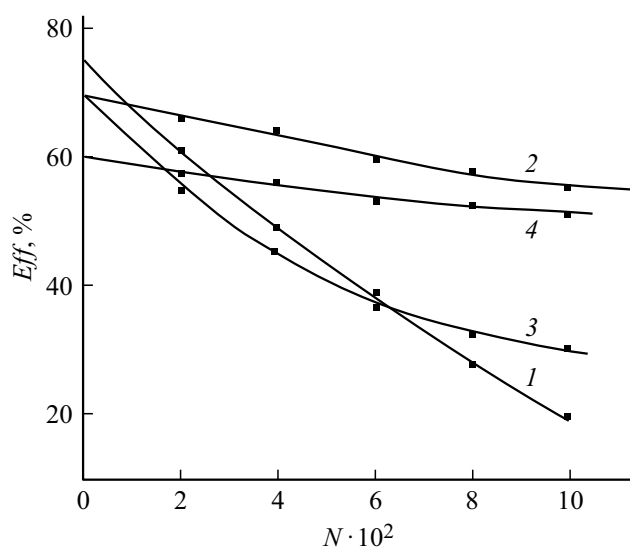


**Figure 13.** Dependence of the efficiency of generation of R6G (1) and phenalemine 160 (3) and their inclusion complexes  $\beta$ -CD (2, 4) on the number of excitation pulses in the water-ethanol solution.

cyclodextrin in case of their complete or partial intrusion into the macrocycle. This is why at next we studied photoresistance of intercalated dye complexes in water-ethanol solution in case of multiple pulsed exposure to the 2nd harmonics of the  $\text{Nd}^{3+}$ :YAG-laser. The exposure pulse energy was equal to 100 mJ with the pulses duration of 15 ns. Fig. 13 shows the dependence of the generation efficiency of R6G and phenalemine 160 and their inclusion complexes on the number of exposure pulses.

In Fig. 13 we can see that the generation efficiency of water-ethanol solution of R6G and phenalemine 160 (curves 1, 3) falls about three times after exposure to  $10^3$  radiation pulses. At the same time, the generation efficiency of intercalated inclusion complexes of R6G and phenalemine 160 with  $\beta$ -CD falls less than by 10% for the given number of pulses and the efficiency is preserved at the level of 60% (curves 2, 4).

Therefore, the performed studies of spectral and generation properties of R6G, phenalemine 160 and cresyl violet have shown that the formation mechanism of the inclusion complexes refers to entering only of individual functional groups and substitutes of dye molecules into the cavity of  $\beta$ -CD. At that, micellar complexes consisting of several molecules of cyclodextrin and dye molecules, and partially intercalated complexes can be formed. The formation of intercalated complexes allows the increase of the generation efficiency and photoresistance of the studied dyes in water-ethanol solutions.

## Conflict of interest

The authors declare that they have no conflict of interest.

## References

- [1] B.C. Burdet. Stud. Phys. Theor. Chem. **26**, 241–270 (1983).
- [2] S.S. Anufrik, S.N. Anuchin. *Optika i spetsktroskopiya kondensirovannykh sred* (materialy XXIV Mezhdunarodnoi nauchnoi konferentsii, Krsanodar), (KubSU, Krasnodar, 2018) (in Russian), research editors V.A. Isaeva, A.V. Lebedeva, V. 1, P. 123–129.
- [3] L.V. Levshin, A.M. Saletskiy, V.I. Yuzhakov. Kvant. elektron., **10** (7), 1413–1419 (1983) (in Russian)
- [4] M.M. Asimov, V.P. Chuev, S.N. Kovalenko, V.M. Nikitchenko, A.N. Rubinov. Opt. i spektr., **70** (3), 544–546 (1991) (in Russian).
- [5] M.A. Kapustin, A.S. Chubarova, T.N. Golovach, V.G. Tsygankov, A.M. Bondaruk, V.P. Kurchenko. Trudy BGU, **11** (1), 73–100 (2016) (in Russian)
- [6] M.M. Asimov, V.P. Chuev, S.N. Kovalenko, V.M. Nikitchenko, A.N. Rubinov, O.D. Kameneva, S.G. Stepanyan. Kvant. elektron., **18** (11), 1308–1310 (1991) (in Russian)
- [7] V.V. Tarkovskiy, S.S. Anufrik. Opt. i spektr., **105** (5), 794–800 (2008) (in Russian)
- [8] M.M. Asimov, B.A. Bushuk, M.A. Senyuk, A.P. Stupak, A.N. Rubinov. Zhurn. prikl. spektr., **66** (5), 619–622 (1999) (in Russian)
- [9] E. Sabadini, T. Cosgrove, F.D.C. Egidio. Carbohydrate Research, **341** (2), 270–274 (2006).
- [10] S.K. Das, R. Rajabalaya, S. David, N. Gani, J. Khanam, A. Nanda. Research Journal of Pharmaceutical, Biological and Chemical Sciences, **4** (2), 1694–1720 (2013).
- [11] K. Frumming, J. Szejtli. Cyclodextrins in Pharmacy (Kluwer Academic Publishers, Dordrecht-Boston, 1994).
- [12] S.S. Anufrik, S.N. Anuchin, V.V. Tarkovskiy. Baltiyskiy morskoy forum. *Innovatsii v nauke, obrazovanii i predprinimatelstve-2018 (materialy VI Mezhdunarodnogo Baltiyskogo morskogo foruma, XVI Mezhdunarodnoy nauchnoy konferentsii, Kaliningrad)*, (BGARF, Kaliningrad, 2018) (in Russian), research editors V.A. Volkogon, N.A. Kostrikova, et al. V. 1, P. 11–20.
- [13] T.A. Andreeva, M.E. Bedrina. Vestnik of SPbGU, **10** (1), 16–24 (2015).
- [14] M. Majoube, M. Henry. Spectrochimica Acta, **41A** (9/10), 1459–1466 (1991).
- [15] *Spravochnye tablitsy osnovnykh spektroskopicheskikh dannykh (IK-, UF-, YaMR-spektroskopiya y mass-spektroskopiya)* (KOKh KhF BGU, Minsk, 2001) (in Russian)
- [16] A.F. Abramov, S.S. Anufrik, G.R. Ginevich, V.A. Mostovnikov, A.N. Rubinov. Zhurn. prikl. spektr., **6** (25), 10–22 (1977) (in Russian)
- [17] G.E. Krichevskiy. *Fotokhimicheskie prevrashcheniya krasitelei i svetostabilizatsiya okrashennykh materialov* (Khimiya, M., 1986) (in Russian)
- [18] V.V. Tarkovskiy, S.S. Anufrik. Opt. i spektr., **105** (5), 794–800 (2008) (in Russian)